A Density Functional Theory Study of η^2 Acyl Bonding in Fe and Mn Carbonyl Complexes

Xianghuai Wang and Eric Weitz*

Department of Chemistry, Northwestern University, Evanston, Illinois 60208-3113

Received: June 12, 2002; In Final Form: August 29, 2002

The stability of the η^2-acyl−Fe(CO)$_3$X (acyl = CH$_3$C(O), C$_2$H$_5$C(O), C(CH$_3$)$_3$C(O); X = H, I, CH$_3$) complexes relative to the respective η^1-acyl−Fe(CO)$_3$X complex and their alkyl isomers has been studied using density functional theory (DFT). The effect of an acetyl versus a propionyl group, and the effect of the nature of the substituent, X, on the stability of various isomers is considered. For the CH$_3$ substituent the effect of a t-valeryl ((CH$_3$)$_3$CC(O)) group was also probed. The η^2-(CH$_3$)$_3$CC(O)Fe(CO)$_3$CH$_3$ complex is the most stable of the iron complexes studied. The effect of the substituents on the energies of the molecular orbitals of the complexes provides insight into the energy ordering of the various isomeric structures. DFT calculations were also performed on the η^2-CH$_3$C(O)Mn(CO)$_4$ complex and its isomers. Good agreement is achieved with regard to these calculations and available experimental and theoretical data. Predictions are presented for the stability of η^2-acyl−Cr complexes.

I. Introduction

The migration of an alkyl group to form an acyl complex is the key step in a number of homogeneous catalytic reactions.[1] The acyl−metal bond can involve either an η^1 or an η^2 interaction.

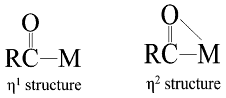

Because the η^2 interaction involves the vacant coordination site that results from alkyl migration, this structure can alter the reactivity of the acyl complex versus an η^1 structure by affecting the rate and energetics of back-migration of the alkyl group.[2] A variety of compounds with η^2 structures have been synthesized and characterized. These include complexes of the group 4 metals, the actinides and other metals, such as V, Mo, W, Mn, Fe, Ru, and Co.[2−5] Recent work by Ford et al., on metal carbonyl alkyl complexes, indicates that both the η^1 and η^2 structures could play a role in the reactivity of CH$_3$C(O)Mn(CO)$_4$.[6]

There has also been considerable theoretical interest in acyl complexes. In 1978 Becke and Hoffmann[7] used an extended Hückel method (EHM) to study the η^1 and η^2 isomers of CH$_3$C(O)Mn(CO)$_4$. Tatsumi et al.[8] used the EHM to study CO insertion into Cp$_2$MRX (M = Ti, Zr, U; R = CH$_3$, C$_6$H$_5$CH$_2$; X = Cl, CH$_3$) complexes to form the corresponding Cp$_2$M(COR)X complex, with the result that the CO bond gets slightly stronger on going from an η^1 to an η^2 structure. Ziegler et al. have done considerable theoretical work on the η^2 structures of acyl−Co,[9] acyl−Mn,[10] and acyl−Pd[11] complexes. In their LCAO−HFS calculation for the acyl−Co complexes,[9a] they concluded that in the η^2 complex the lone pair of the O interacts with the Co atom. Rappé[12] used the generalized valence bond (GVB) approach to calculate the η^2 structure of HC(O)ScCl$_2$ and also showed that the O lone pair interacted with the empty d orbital of Sc. This interaction is also evident in our current study of η^2-acyl−Fe complexes. An ab initio study of the complete alkyl migration pathway in an actual organometallic system was published 15 years ago by Axe and Marynick[13] who used PRDDO and HF calculations to treat the Mn(CO)$_5$CH$_3$ system. Another early study of this system was published by Ziegler et al.[10] Recently, Derecskei-Kovacs and Marynick (DM) reported on the potential energy surface for the carbonylation of Mn(CO)$_5$CH$_3$ and the decarbonylation of CH$_3$C(O)Mn(CO)$_5$.[14] In ref 14, CH$_3$Mn(CO)$_5$ was calculated to be more stable than η^2-CH$_3$C(O)Mn(CO)$_4$ and the η^1-CH$_3$C(O)Mn(CO)$_4$ complex was found to be a transition state between the η^2 complex and a species in which there is an agostic interaction between the methyl group and the open site on Mn.

Experimental studies of reactions that take place after formation of a (C$_2$H$_5$I)Fe(CO)$_4$ complex as a result of the reaction of C$_2$H$_5$I with Fe(CO)$_4$ have recently been performed in our laboratory.[15] Several low activation energy processes follow the initial association step. Oxidative addition of C$_2$H$_5$I to Fe(CO)$_4$ can lead to the formation of isomers of C$_2$H$_5$Fe(CO)$_4$I, including new acyl complexes. As such, there is little or no relevant literature data that would allow us to assign observed infrared absorptions, obtained from our transient infrared spectroscopy experiments, to a specific isomer. Therefore, we performed calculations of the energies and carbonyl stretching frequencies of various possible intermediates in this system to allow us to assess the likelihood that a given C$_2$H$_5$Fe(CO)$_4$I isomer plays a role in the reaction pathways that have been observed.

To obtain insights into the effect of alkyl chain length and substituents on the energy of such complexes, calculations were performed for the η^2 versus the η^1 isomers of RFe(CO)$_4$X (R = CH$_3$, C$_2$H$_5$, X = I, H, CH$_3$). For CH$_3$C(O)Fe(CO)$_3$I the energy of the η^2 isomer is close to the energy of the η^1 isomer. However, for CH$_3$C(O)Fe(CO)$_3$H the η^2 structure is significantly lower in energy than that of the η^1 structure. The energies of the molecular orbitals (MOs) of the various acyl−Fe isomers provide insight into the energetics of the η^2 structure versus the η^1 structure of CH$_3$C(O)Fe(CO)$_3$H.

Calculations were also performed on CH$_3$Mn(CO)$_5$ and its isomers for which both experimental and theoretical data are

10.1021/jp0214099 CCC: $22.00

TABLE 1: Calculated Reaction Enthalpy (kcal/mol) for Reactions Involving $CH_3Mn(CO)_5$ Isomers

	BLYP	BP86	Ziegler et al.[a]	Axe et al.[b]	Kovacs et al.[c]
$(\eta^1\text{-}CH_3CO)Mn(CO)_4 \rightarrow (\eta^2\text{-}CH_3CO)Mn(CO)_4$	−15.46	−16.45	−19	−11	−17.6
$(\eta^1\text{-}CH_3CO)Mn(CO)_4 \rightarrow CH_3Mn(CO)_5$	−22.72	−23.74	−18	−10	−23.1
$(\eta^1\text{-}CH_3CO)\,Mn(CO)_4 + THF \rightarrow$ *cis*-$CH_3C(O)Mn(CO)_4(THF)$	−33.26[d]	−36.00[d]			
	−27.60[e]	−30.99[e]			

[a] Reference 10, calculation based on HFS model. [b] Reference 13, with an ab initio HF calculation. [c] Reference 14, with a DFT/B3LYP calculation. [d] Without the BSSE correction. [e] With the BSSE correction.

available. Predictions are also made regarding the energetics of some η^2 acyl−Cr carbonyl complexes.

II. Computational Methods

The majority of the DFT calculations were performed using the Jaguar quantum chemistry program.[16] For Cr and Fe complexes the Slater local exchange functional,[17] Becke's 88 nonlocal gradient correction[18] to exchange, and Perdew's[19] gradient correction functional for the Vosko−Wilk−Nusair (VWN)[20] local correlation functional (BP86) was used. For Mn-containing molecules, BP86, B3LYP, and BLYP were used. BLYP used the Slater local exchange functional,[17] Becke's 88 nonlocal gradient correction[18] to exchange, and the Lee−Yang−Parr[21] nonlocal correlation functional. B3LYP used the exact HF Slater local exchange functional,[17] Becke's 88 nonlocal gradient correction[18] to exchange, and the VWN local functional, and the Lee−Yang−Parr local and nonlocal functionals.[21] The LACV3P** basis set[22] was employed. It has an effective core potential (ECP) for Cr, Mn, and Fe and uses the 6-311G** basis set for atoms from H to Ar. The LAV3P basis set,[22] which also contains an ECP, was used for I. Within these basis sets (LACV3P** and LAV3P), the 6-31G basis set was used to describe the bonding orbitals (3s, 3p, 4s, 3d, 4p for Cr, Mn, and Fe and 5s, 5p for I).

The reaction enthalpy at 298.15 K can be calculated by the expression[23]

$$\Delta H_{298.15} = \Delta E + \Delta \mathrm{ZPE} + \Delta E_{\mathrm{th}} + \mathrm{BSSE} + \Delta(PV) \quad (1)$$

Here Δ is defined as the difference between the calculated quantity for the products and the reactants in a given reaction. Thus, ΔE is the change in the optimized energy, ΔZPE is the difference in the zero-point vibrational energy, ΔE_{th} is the difference in the thermal energy content, which is the sum of the changes in translational, rotational, and vibrational energy when going from 0 to 298.15 K. Δ(PV) is the molar work term, which assuming ideal gas behavior, is equal to $(\Delta n)RT$, where Δn is the difference in the number of moles of the products and the reactants. The basis set superposition error (BSSE) correction is obtained by running a counterpoise calculation.[24] The BSSE is only considered in calculations of bond dissociation energies (BDEs): There should be very little difference in the basis set superposition error in the calculation of the relative energy of isomers of a given complex. The BSSEs calculated for the relevant Fe and Cr complexes were ∼1−2 kcal/mol. The BSSEs for the Mn complexes were somewhat larger: ∼5 kcal/mol.

In prior DFT calculations[25] on the Fe and Cr containing complexes it was shown that among the B3LYP, BLYP, and BP86 functionals, the BP86 functional provided the best match to experimentally determined bond energies. Thus, we have used the BP86 functional in our calculation for Fe- and Cr-containing complexes.

The BLYP, B3LYP, and the BP86 functionals were all used to calculate the BDE for the Mn−H bond in $HMn(CO)_5$,

$$HMn(CO)_5 \rightarrow H + Mn(CO)_5 \quad (2)$$

They gave BDEs of 57.99 kcal/mol (DFT/BLYP), 59.57 kcal/mol (DFT/B3LYP), and 62.64 kcal/mol (DFT/BP86). These values can be compared to experimental values for this BDE of 68 ± 1,[26] 65,[27] 51 ± 2,[28] and 63[29] kcal/mol. As a result of the significant variation in experimental data and the similarity in calculated values, these experimental data cannot be used to convincingly conclude which functional provides the best agreement. As such, additional calibration calculations were performed for the reaction

$$CH_3Mn(CO)_5 + CO \rightarrow Mn(CO)_5(COCH_3) \quad (3)$$

for which there is an experimental value of 8.0 ± 1.4 kcal/mol[14] for the enthalpy change. Using Jaguar and the BLYP, B3LYP, and BP86 functionals, the enthalpy change (including the BSSE correction) for the above reaction was calculated. The BLYP functional gives a result (6.52 kcal/mol) that is virtually within the reported experimental error. The B3LYP functional gives a result (5.59 kcal/mol) that does not deviate significantly from the reported value, and the BP86 functional gives a significantly larger value (13.84 kcal/mol). Neglecting the BSSE correction gives larger calculated enthalpy changes that are even closer to the experimentally reported value for both BLYP and B3LYP, but further away from the experimental value for BP86. As such, we concluded that the BLYP functional is likely to give the best results for acyl−Mn complexes. However, we felt it would be instructive to perform calculations using both the BP86 and BLYP functionals to ascertain the range of differences in calculated energies for the Mn complexes studied. As will be seen, perhaps surprisingly, though the calculations using the BLYP and BP86 functionals (shown in Table 1) gave somewhat different energies, the energy *difference* among the $(\eta^2\text{-}CH_3CO)Mn(CO)_4$, $(\eta^1\text{-}CH_3CO)Mn(CO)_4$, and $CH_3Mn(CO)_5$ species were often very *similar independent of which of these functional was used*. Though energy differences between some species are of a magnitude comparable to that expected for the uncertainty in the calculated value, as we have done previously, we focus on trends in energies among the species considered.[30]

Calculations were also performed to determine the minimum energy structure of $\eta^1\text{-}CH_3C(O)Mn(CO)_4$ using the Amsterdam density functional theory (ADF) program[31] and the same BLYP functional as used in the Jaguar calculations. The triple-ζ STO basis set was used for all atoms with a polarization function added for H, C, and O atoms.[32] The $1s^22s^22p^6$ configuration of Mn and the $1s^2$ configuration of H, C, and O were assigned as the core and treated within the frozen core approximation.[31b]

III. Results and Discussion

A. Calibrations and Enthalpies of η^1- and η^2-$CH_3C(O)Mn(CO)_4$ Complexes.

Ford et al.[6] have published a number of studies of the $CH_3C(O)Mn(CO)_4$ system. Some experimental observations are explained in terms of the chelated acyl complex, (η^2-CH_3CO)$Mn(CO)_4$, being present in weakly coordinating solvents such as cyclohexane.[6] However, if the solvent is sufficiently strongly coordinating, Ford et al. hypothesize that a "solvento complex" can form from the η^1 isomer, which can effectively "lock-out" the η^2 isomer of $CH_3C(O)Mn(CO)_4$.

Derecskei-Kovacs and Marynick have recently published a theoretical study of the potential energy surface for the carbonyl insertion reaction for $CH_3Mn(CO)_5$.[14] DM agree with previous work[10,13] that the η^2 species is lower in energy than the η^1 complex. However, they indicate that rather than being a local minimum on the potential energy surface for the system the η^1 complex is a transition state between the η^2 complex and an isomer in which there is an agostic interaction between a hydrogen on the methyl group and the metal center. Both of these interactions (agostic and η^2) effectively block the open site produced as a result of methyl migration to form the acyl moiety.

As a result of these reports, and as a complement to our calculations on Fe acyl complexes, we performed calculations on the Mn complexes of relevance to alkyl migration reactions studied by Ford et al.[6] and to the calculations performed by Derecskei-Kovacs and Marynick.[14]

Our calculated enthalpy difference (Table 1) between η^2-$CH_3C(O)Mn(CO)_4$ and $CH_3Mn(CO)_5$ is 7.26 kcal/mol (BLYP), which is in good agreement with the recent work by DM.[14] They calculated the enthalpy difference to be 5.5 kcal/mol using the B3LYP functional and the larger of their basis sets. On the basis of the equilibrium constant between $CH_3Mn(CO)_5$ and η^2-$CH_3C(O)Mn(CO)_4$, Ford et al.[6a] estimated, on the basis of data in ref 33, that the free energy difference between $CH_3Mn(CO)_5$ and η^2-$CH_3C(O)Mn(CO)_4$ is 8.9 kcal/mol, with the former species being more stable. Using a calculated value for the entropy, we calculated the free energy of η^2-$CH_3C(O)Mn(CO)_4$ to be 9.52 kcal/mol (BLYP) higher than that of $CH_3Mn(CO)_5$. This energy difference is very close to the value of 8.9 kcal/mol given by Ford et al.[6a]

To further test our results versus those in ref 14, we performed a calculation for the η^1 structure that DM found to be a transition state. Their exact structure gave multiple negative frequencies in our calculation. As such, we ran a transition state search using this structure as an initial guess. The structure of the resulting transition state, which has one negative (imaginary) frequency, was very similar to the structure of the transition state calculated by DM: the largest difference in bond distances was less than 0.001 A and the largest difference in bond angle was less than 0.1°, effectively the same structure. We also calculated the energy difference between this species and their optimized structure for the η^2 species as 17.5 kcal/mol (BLYP), which is very similar to their calculated value of 17.6 kcal/mol.

However, in our calculations we found an alternative η^1 structure that can be optimized to a local minimum. The structure is shown below and its geometric parameters are presented in Table 2. It is 13.09 kcal/mol (BLYP) less stable than our calculation of the energy of the η^2 structure of this complex that was calculated by DM.[14] As a further check that this alternative η^1 structure is a minimum it was verified that all frequencies were real. Calculations using the B3LYP functional, which was employed in ref 14, gave similar results. Additionally, an optimization of this structure using ADF gave a minimum energy η^1 structure that was quite similar to that calculated with Jaguar. Frequencies were also calculated with ADF to ensure they were all real. However, it should be noted that in all of these calculations the potential around the minimum was very shallow: between 1 and 2 kcal/mol.

TABLE 2: Calculated Geometry[a] for (η^1-CH_3CO)$Mn(CO)_4$ and (η^2-CH_3CO)$Mn(CO)_4$ Using BP86 and BLYP Functionals

	(η1-CH3CO)$Mn(CO)_4$		(η^2-CH_3CO)$Mn(CO)_4$	
	BP86	BLYP	BP86	BLYP
Mn1−C2	1.946	1.982	1.919	1.949
Mn1−C8	1.889	1.918	1.842	1.868
Mn1−C10	1.821	1.848	1.785	1.812
Mn1−C12/Mn1−C14	1.846	1.873	1.850	1.878
C8−O9	1.152	1.153	1.156	1.157
C12−O13/C14−O15	1.156	1.157	1.155	1.156
C10−O11	1.161	1.162	1.162	1.163
C2−O3	1.215	1.218	1.235	1.238
C2−C4	1.526	1.540	1.489	1.502
C4−H	1.097	1.098	1.099	1.100
O3−C2−Mn1	116.5	116.8	84.2	85.1
C4−C2−Mn1	121.7	121.9	150.3	150.0
O13−C12−Mn1/ O15−C14−Mn1	176.7	177.5	176.8	177.6
O9−C8−Mn1	173.8	173.3	178.2	177.7
O11−C10−Mn1	174.1	173.5	178.4	178.2
C2−Mn1−C8	96.6	96.7	147.2	147.5
C2−Mn1−C10	100.9	101.2	111.9	111.2
C2−Mn1−C12/ C2−Mn1−C14	86.9	87.5	89.7	89.3

[a] Bond lengths in Å, angle in degree.

The enthalpy (ΔH) for the reaction:

$$\eta^1\text{-}CH_3C(O)Mn(CO)_4 \rightarrow \eta^2\text{-}CH_3C(O)Mn(CO)_4 \qquad (4)$$

was calculated as −15.46 kcal/mol (see Table 1) using the BLYP functional. Our calculated minimum energy η^2 structure is shown below and its geometric parameters are presented in Table 2. This η^2 structure is very similar to the optimized η^2 structure obtained by DM.

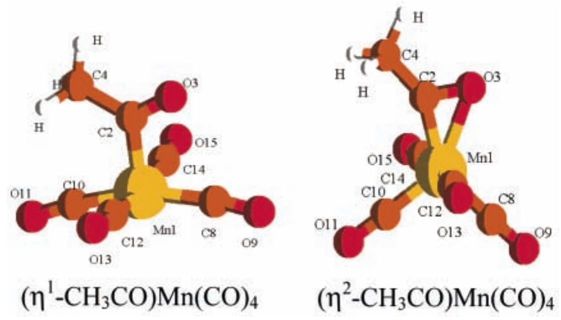

(η^1-CH_3CO)$Mn(CO)_4$ (η^2-CH_3CO)$Mn(CO)_4$

Our calculation of the energy of both structures using our basis set and the BLYP functional gave the result that our optimized structure is 2.07 kcal/mol more stable than the structure presented by DM. The difference in the structures is sufficiently minor that it is plausible that the small difference in the calculated energies are not due to intrinsic physical differences between these structures but to differences in calculational methodology, i.e., the structure we calculate and the structure calculated by DM represent the same chemical species. However, because our structure for this complex is the optimized minimum energy structure for our basis set and functional, it will by necessity give a lower energy than the optimized structure determined by DM, even if these structures effectively represent a common chemical species.

Even a transiently stable η^1 structure would leave open the possibility that such a species is transiently present in solution and thus it could interact with a coordinating solvent forming

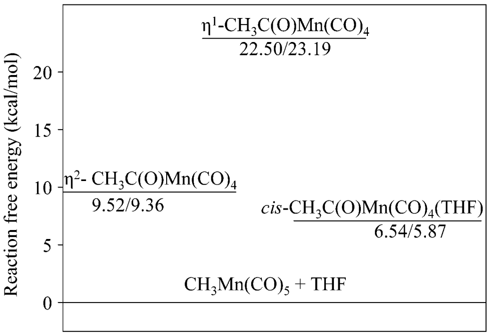

Figure 1. Relative free energies of relevant acyl−Mn complexes. Free energies are referenced to $CH_3Mn(CO)_5$ + THF. The free energies indicated below the complexes were calculated with the BLYP and BP86 functionals, respectively.

a solvento complex. However, we point out that the existence of a transiently stable η^1 complex does not guarantee formation of a solvento complex. That of course depends on the shape of the potential energy surface for the system and microscopic details of the operative kinetics. Nevertheless, we also calculated the BDE for THF interacting with the vacant site of the η^1 complex shown above.

The reaction enthalpy for

$$(\eta^1\text{-}CH_3CO)Mn(CO)_4 + THF \rightarrow cis\text{-}CH_3C(O)Mn(CO)_4(THF) \quad (5)$$

was calculated using the BLYP functional as −27.60 kcal/mol when the BSSE correction is included. The BSSE correction for both the BLYP and the BP86 functionals are relatively large: 5.66 and 5.01 kcal/mol, respectively (see Table 1). We note that if these terms overestimate the BSSE correction, the BDE for the THF complex will be larger. *cis*-$CH_3C(O)Mn(CO)_4(THF)$ is used in eq 5 because it is 9.6 kcal/mol more stable than *trans*-$CH_3C(O)Mn(CO)_4(THF)$.

Another conclusion from the experimental data in ref 6a is that $CH_3Mn(CO)_5$ is more stable than η^2-$CH_3C(O)Mn(CO)_4$. Both the recent work by DM and our calculations agree that this is the case. The calculated relative free energies for these complexes and the *cis*-$CH_3C(O)Mn(CO)_4(THF)$ complex are shown in Figure 1.

Ford indicates in ref 6a that there is a 5.5 kcal/mol free energy difference between the complex on the right-hand side of eq 5 and the more stable $CH_3Mn(CO)_5$ complex. Our calculation of the free energy difference between $CH_3C(O)Mn(CO)_4(THF)$ and $CH_3Mn(CO)_5$ is 6.54 kcal/mol (BLYP), which is consistent with Ford's value. On the basis of a comparison of the relative free energy of *cis*-$CH_3C(O)Mn(CO)_4(THF)$, η^2-$CH_3C(O)Mn(CO)_4$, and $CH_3Mn(CO)_5$, which are shown in Figure 1, we can conclude that if the solvento species, *cis*-$CH_3C(O)Mn(CO)_4(THF)$, forms it would be expected to be of lower free energy than η^2-$CH_3C(O)Mn(CO)_4$.

B. η^2-Acyl−Fe Complexes. Calculations of the structure of $C_2H_5Fe(CO)_4I$ converged to four geometrical isomers: *trans*-$C_2H_5Fe(CO)_4I$, *cis*-$C_2H_5Fe(CO)_4I$, η^2-$C_2H_5C(O)Fe(CO)_3I$, and η^1-$C_2H_5C(O)Fe(CO)_3I$ (Chart 1). In each case we consider the lowest energy conformational isomer for the indicated geometrical isomer (i.e., trans, cis, η^1, and η^2). The energies of these four isomers are listed in the second row of Table 3 and are shown in Figure 2, from which it can be seen that the cis isomer is the most stable. Though the energy differences between these isomers are small, and within the range of expected calculational errors, we concentrate on the trend in the energies of these species.[25]

CHART 1

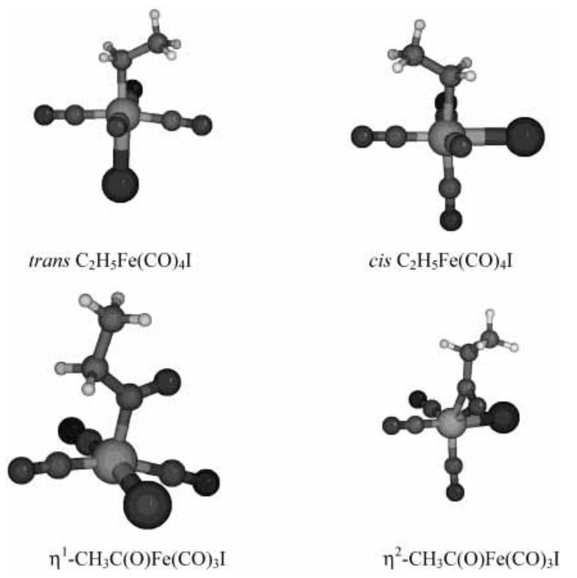
trans $C_2H_5Fe(CO)_4I$ *cis* $C_2H_5Fe(CO)_4I$

η^1-$CH_3C(O)Fe(CO)_3I$ η^2-$CH_3C(O)Fe(CO)_3I$

TABLE 3: Relative Stability[a,b] of the Isomers of Acyl−Fe Complexes

	trans	cis	η^2	η^1
$CH_3Fe(CO)_4I$		−5.09	−1.22	0
$C_2H_5Fe(CO)_4I$	1.91	−1.79	−1.18	0
$CH_3Fe(CO)_4H$		−16.10	−8.56	0
$C_2H_5Fe(CO)_4H$		−14.21	−8.94	0
$CH_3Fe(CO)_4CH_3$		−11.16	−5.32	0
$C_2H_5Fe(CO)_4CH_3$		−8.23	−7.54	0
$(CH_3)_3CFe(CO)_4CH_3$	1.29	−1.35	−9.23	0

[a] Energies in kcal/mol. [b] The energy of the η^1 structure is set to zero and the energies of the other structures are reported relative to the η^1 structure.

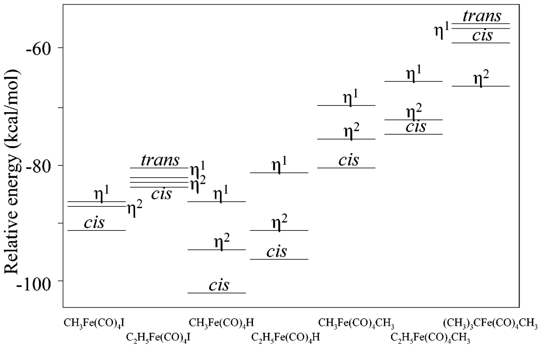

Figure 2. Relative energies of relevant acyl−Fe complexes where the parent complexes are indicated along the abscissa. The energy origin for each structure corresponds to the separated alkyl radical, substituent, and $Fe(CO)_4$ moieties.

It is clear from the literature that the nature of the alkyl group can affect the kinetics of alkyl migration reactions. In a study of the influence of the alkyl chain length on the migration rate in $RMn(CO)_5$ complexes, Anderson et al.[34] concluded that the rate of alkyl migration increases from methyl to *n*-propyl and then decreases from *n*-butyl to *n*-heptyl because of the steric effects, and there is a continuing slow decreases from *n*-octyl to larger alkyl groups. However, it is not clear how the nature of the alkyl group or other substituents bound to a metal center affect the energetics of the different isomers of a given complex. The term substituent (indicated as X) is used in this context to indicate a one-electron donating ligand that does not directly participate in the alkyl migration process. Calculations were performed for $RC(O)Fe(CO)_3X$ species with R = CH_3, C_2H_5, and X = I, H, and CH_3. Because the energy of the trans structure is always higher than that of the cis structure, we concentrated on the lower energy isomers that we expect to play a role in the alkyl migration process. These are the cis, η^2, and η^1 structures.

The energies of the C_2H_5 analogues of the CH_3 complexes were also calculated. The results of these calculations are shown in Table 3 and in Figure 2. There is little change in the energy difference between the η^2 and η^1 structures between the R = CH_3 and the R = C_2H_5 complexes, but the relative energy of the cis to η^1 structure changes somewhat more. Our calculations also show that the alkyl−metal BDE can change significantly. The BDE for $C_2H_5{-}Fe(CO)_4I$ is 30.68 kcal/mol, which is smaller than the BDE for $CH_3{-}Fe(CO)_4I$, of 38.55 kcal/mol. The weaker metal−C_2H_5 bond would be expected to facilitate the alkyl migration process for this complex. The BDEs for the alkyl group−CO bond in the acyl moiety were also calculated. The BDE for $CH_3{-}C(O)Fe(CO)_3I$ is 31.51 kcal/mol, whereas the BDE for $C_2H_5{-}C(O)Fe(CO)_3I$ is 28.41 kcal/mol. Thus, a change in the alkyl group from CH_3 to C_2H_5, has a larger effect on the energy of the alkyl−Fe bond than it has on the energy of the alkyl−CO bond. On the basis of these results a relatively small difference in the BDEs for the $C_2H_5C(O){-}Fe(CO)_3I$ and the $CH_3{-}C(O)Fe(CO)_3I$ bonds would also be expected. The conversion of a cis isomer to the corresponding η^1 isomer can be viewed as breaking a metal−alkyl and metal−CO bond and forming an alkyl−CO and a metal−acyl bond. In the context of this picture and the above discussion, a weaker alkyl−Fe bond would be expected to lead to the energy of the cis isomer being closer to or even larger than the energy of the η^1 isomer.

We also investigated the effect of a change from an I atom substituent to an H atom in these complexes. The energies obtained for both alkyl groups (CH_3 and C_2H_5) with H as a substituent are listed in the third and fourth rows of Table 3, respectively. The energy difference between the cis isomer and the η^1 structure decreases for C_2H_5 relative to CH_3. Another interesting observation is that the energy *difference* between the cis isomer and the η^1 structure decreases for I relative to H for both alkyl groups (see Table 3). Additionally, the energy difference between the η^1 and η^2 isomers changes significantly when H is substituted for I. The η^2 isomer is the more stable of the two for $C_2H_5C(O)Fe(CO)_3H$ and $CH_3C(O)Fe(CO)_3H$; however, the cis isomer is still the most stable structure for both complexes. In the next section, we consider the energies of the molecular orbitals (MOs) of the various complexes to obtain insights into changes in the relative energies of the η^1 and η^2 isomers as a function of substituent.

Also shown in Table 3 are the energies for the various isomers of the $CH_3Fe(CO)_4CH_3$, $C_2H_5Fe(CO)_4CH_3$, and $(CH_3)_3CFe(CO)_4CH_3$. For the H analogues of these complexes there is little change in the relative energies of the cis and η^2 isomers for an ethyl versus a methyl. However, for all of the aforementioned complexes there is a significant change in the relative energies of the cis to η^2 isomers when the alkyl group is larger. For methyl and ethyl the cis isomer is lower in energy than the η^2 isomer, though for the ethyl complex the difference in energy is less than 1 kcal/mol. However, for the *tert*-butyl complex the η^2 isomer, which is the most stable isomeric structure of this complex, is significantly more stable than the cis isomer (see Table 3).

TABLE 4: Relationship between the CFeO Angle and the Relative Energy of the η^2 Structure to the η^1 Structure

	∠CFeO (deg)	energy of $\eta^1 \rightarrow \eta^2$ (kcal/mol)
$CH_3CO{-}Fe(CO)_3I$	34.470	−1.22
$C_2H_5CO{-}Fe(CO)_3I$	34.445	−1.18
$CH_3CO{-}Fe(CO)_3H$	34.904	−8.56
$C_2H_5CO{-}Fe(CO)_3H$	34.889	−8.99
$CH_3CO{-}Fe(CO)_3CH_3$	34.593	−5.32
$C_2H_5CO{-}Fe(CO)_3CH_3$	34.608	−7.54
$(CH_3)_3CCO{-}Fe(CO)_3CH_3$	34.633	−9.23

TABLE 5: Unscaled Calculated CO Vibrational Frequencies of $C_2H_5Fe(CO)_4I$ Isomers

	CO vibrational frequencies (cm^{-1})			
trans	2033	2036	2057	2109
cis	2029	2041	2050	2102
η^1	1735	2001	2021	2085
η^2	1659	2010	2029	2079

We note that the $(CH_3)_3C{-}Fe$ bond length in *cis*-$(CH_3)_3CFe(CO)_3CH_3$ is 2.352 Å, whereas the $C_2H_5{-}Fe$ bond in *cis*-$C_2H_5Fe(CO)_3CH_3$ is 2.170 Å. The much longer bond length for the $(CH_3)_3C$ complex versus the C_2H_5 complex is compatible with the smaller BDE that has been calculated for the former complex relative to the latter (vide infra). This result is not surprising because the greater steric interactions that would be expected as the $(CH_3)_3C$ moiety approaches the unsaturated $Fe(CO)_3CH_3$ species would be expected to lead to a longer bond than when the smaller C_2H_5 moiety approaches $Fe(CO)_3CH_3$. A similar effect was seen in the bonding of substituted olefins to $Cr(CO)_5$.[35] With everything else being equal, a decrease in the degree of orbital overlap would be expected to lead to a weaker metal−alkyl bond. Of course, everything else is not necessarily equal and in the next section we consider a molecular orbital approach that includes the effect of both the energies and overlaps of the interacting orbitals.

The C−Fe−O angle in the η^2-alkyl−C(O)−Fe complexes also contains information on the relative stability of the η^2 structure compared to its isomers. In ref 13, Axe and Marynick pointed out that although the η^2 interaction seems to be electronically favorable, strain in the metallacycle acts to increase the energy of the complex. The C−Fe−O angles in the complexes we consider are listed in Table 4. From the table it is apparent that in agreement with Axe and Marynick, for a given substituent, the larger the angle the more stable the η^2 structure is relative to the η^1 isomer. Additionally, for a given substituent (H, I, CH_3) a larger angle correlates with a relatively more stable η^2 structure for that series of complexes. Inspection of these data also makes it clear that the absolute value of the angle is more strongly influenced by the substituent than by the nature of the alkyl group in the acyl moiety. The unscaled calculated carbonyl stretching frequencies are listed in Table 5.

C. Relationship to Experimental Data on $(C_2H_5)Fe(CO)_4I$ Complexes. Transient infrared spectroscopy has been used to study the interaction of $Fe(CO)_4$ and C_2H_5I.[15] The signals obtained in these experiments indicate that multiple species form as a result of reaction processes that take place after the reactive interaction of $Fe(CO)_4$ and C_2H_5I, which involves an oxidative addition process. With the experimental conditions employed, the species thus formed are expected to be isomers of $C_2H_5Fe(CO)_4I$, and CO adducts of the unsaturated acyl isomers in this system. Because equilibria between isomers of similar energy are possible, and would lead to a larger equilibrium concentration of the lower energy isomer, the relative energies of different isomers in the system can be an aid in constructing a plausible kinetic model and ultimately in the assignment of

CHART 2

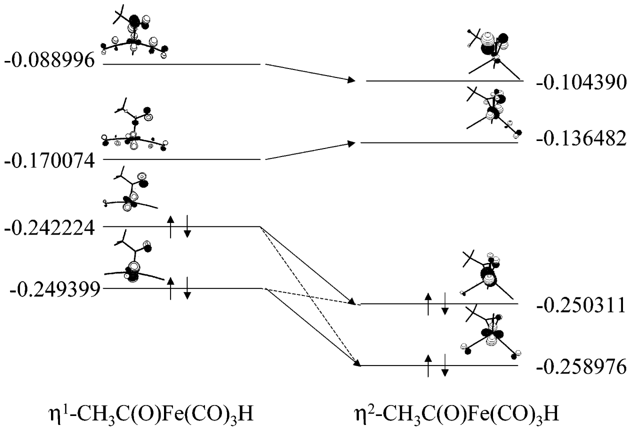

specific transients. Similarly, calculated frequencies can help confirm assignments. Such data are particularly valuable in systems, such as the present, in which there is both no available spectroscopic data for possible transient species and no clear prior quantitative expectation as to the relative energies of different isomeric species. The absence of such data motivated our theoretical study of these complexes. The details of the experiments, the modeling of the kinetics of this reaction system, conclusions regarding assignments of observed transient infrared signals to specific species and reaction processes, and how the calculations reported in the present work were utilized will be reported on in a separate publication.[15]

D. Molecular Orbitals of the Acyl−Fe Complexes. It is interesting to note that the energies of the isomers of $CH_3C(O)Fe(CO)_3I$ are very similar whereas the energies of the isomers of the $CH_3C(O)Fe(CO)_3X$ ($X = H, CH_3$) complexes vary by a greater amount. In Table 1, we see that η^2-$CH_3C(O)Mn(CO)_4$ is significantly more stable than the corresponding η^1 structure. Because I is an electronegative atom, it would be expected to withdraw electron density from the Fe atom in the $CH_3C(O)Fe(CO)_3I$ complex, making this complex the most similar (among $X = H, CH_3, I$), in terms of electron density, to the $CH_3C(O)Mn(CO)_4$ complex which contains the more electron deficient Mn atom. However, our calculations do not support this simple picture. Though the η^2 structure of $CH_3C(O)Fe(CO)_3I$ is more stable than the corresponding η^1 isomer, in contrast to the corresponding Mn complexes, these isomers are of similar energy and much closer in energy than the corresponding Fe complexes with a H substituent ($CH_3C(O)Fe(CO)_3H$) (Table 3). As such, we consider a correlation diagram between the relevant MOs of these two isomers to try to gain insight into the factors that lead to the energy differences in the Fe complexes. A molecular orbital approach has very frequently been used to provide a “chemist’s insight” into the changes in bonding and/or energy levels that occur as a result of a chemical transformation. However, it should be kept in mind that this approach would not be expected to provide precise quantitative bond energies.

The calculated energies for the relevant molecular orbitals of η^1-$CH_3C(O)Fe(CO)_3H$ and η^2-$CH_3C(O)Fe(CO)_3H$ are shown in Chart 2. The highest occupied molecular orbital (HOMO) of η^1-$CH_3C(O)Fe(CO)_3H$ involves the O atom’s lone pair electrons and a hybrid d orbital of Fe. After the formation of η^2-$CH_3C(O)Fe(CO)_3H$, it is apparent there is an increase in electron density in the hybrid d orbital of Fe and a decrease in electron density on the O atom. This is consistent with donation interaction from the O atom to the Fe atom, which stabilizes the η^2 bond. As previously indicated, this interaction between the O lone pair and an orbital of the metal to form the η^2 bond is discussed by Ziegler[9a] and Rappé.[12] Simply looking at the individual orbitals in the η^1 structure, one would conclude that the energy of the second highest occupied MO does not change significantly in going from the η^1 to the η^2 isomer, but the energy of the HOMO changes by a significantly greater amount. These diabatic changes in energy are shown by the dashed lines in Chart 2. However, the two lowest occupied MOs are of the same (A) symmetry and thus the noncrossing rule is operative.[36] In this case, the actual (adiabatic) correlation between the relevant orbitals is shown with bold arrows. From Chart 2 it can be determined that the energy of the electrons in the MOs change by ~22 kcal/mol in going from the η^1 to the η^2 isomer of $CH_3C(O)Fe(CO)_3H$. Note that energies in Charts 2 and 3 are in hartrees, where 1 hartree = 627.5 kcal/mol.

CHART 3

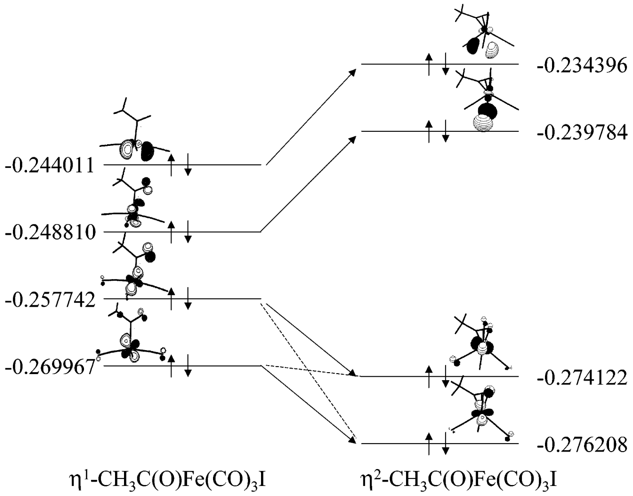

The energies of the relevant orbitals for η^2-$CH_3C(O)Fe(CO)_3I$ and η^1-$CH_3C(O)Fe(CO)_3I$, which are shown in Chart 3, were calculated using Jaguar and the BP86 functional. From the pictures of the molecular orbitals, it is clear that the third and the fourth highest occupied MOs of (η^1-CH_3CO)$Fe(CO)_3I$ are similar to the HOMO and the second highest occupied MO of (η^1-CH_3CO)$Fe(CO)_3H$. Thus, it is not surprising that after (η^2-CH_3CO)$Fe(CO)_3I$ forms, the electrons in these two MOs are lower in energy. Based on the energies calculated for these MOs, this difference is 28 kcal/mol, which is even more than the change involved in going from the η^1 to the η^2 isomer with H as a substituent. From the figure it is also apparent that the HOMO and the second highest occupied MO of η^1-$CH_3C(O)Fe(CO)_3I$ involve mainly the orbitals of the I atom. Though it might not be anticipated that the iodine atom would be involved in the changes in bonding that occur in going from the η^1 to the η^2 structure, it is clear from the pictures in Chart 3 that there is a significant change in electron density, as a result of the isomerization process, that involves both the I and O atoms. The electron density around the I atom is more localized in the η^2 isomer. Formation of η^2-$CH_3C(O)Fe(CO)_3I$, leads to an *increase* in the energy of the electrons in the HOMO and second highest occupied MO by 23 kcal/mol. In comparison to the η^1 and η^2 isomers of $CH_3C(O)Fe(CO)_3H$, even though the energies of the next two lower MOs of $CH_3C(O)Fe(CO)_3I$ decrease in energy, the increase in energy of the two highest occupied molecular orbitals *decreases* the stability of η^2-$CH_3C(O)Fe(CO)_3I$ relative to η^1-$CH_3C(O)Fe(CO)_3I$. Overall, the energies of the electrons in the four MOs shown in Chart 3 decrease by ~5 kcal/mol in going from η^1-$CH_3C(O)Fe(CO)_3I$ to η^2-$CH_3C(O)Fe(CO)_3I$. Thus, the η^1 to η^2 isomerization leads to less of a change in the total energy of the occupied MOs, shown in Charts 2 and 3, for $CH_3C(O)Fe(CO)_3I$ than for $CH_3C(O)Fe(CO)_3H$.

Our DFT calculations demonstrate that the $CH_3{-}Fe(CO)_3CH_3$ BDE of ~41 kcal/mol is greater than the $C_2H_5{-}Fe(CO)_3CH_3$ BDE of ~34 kcal/mol, which is significantly greater than the $(CH_3)_3C{-}Fe(CO)_3CH_3$ BDE of ~18 kcal/mol. This trend is counter to what is expected in terms of the degree of electron density available on the alkyl group, which is expected to increase with increasing chain length.[35] A well known approach to calculating molecular orbital interaction energies takes into account overlap integrals as well as the energies of the interacting oribtals. In this case these oribtals are SOMOs: singly occupied molecular orbitals. For two SOMOs, e_1° and e_2°, involved in bond formation, the orbital interaction energy is[37]

$$\Delta E = \frac{2(\Delta_{12} - e_1^\circ S_{12})^2}{e_1^\circ - e_2^\circ} + e_1^\circ - e_2^\circ \tag{6}$$

where $\Delta_{12} = \langle\psi_1|H|\psi_2\rangle$ and $S_{12} = \langle\psi_1|\psi_2\rangle$. The SOMO energy, e_1°, for $Fe(CO)_3CH_3$ is −0.230 hartrees and the SOMO energies, e_2°, for CH_3, C_2H_5, and $(CH_3)_3C$ are −0.213, −0.185, and −0.156 hartrees, respectively.

The overlap integrals were calculated using ADF[31] and follow the anticipated trend. S_{12}, for methyl, ethyl, and *tert*-butyl with $Fe(CO)_3CH_3$ are 0.31, 0.29, and 0.26, respectively, and $\Delta_{12} = \kappa(e_1^\circ + e_2^\circ)S_{12}/2$ ($\kappa = 1.75$).[38] It is obvious from eq 6 that both the magnitude of the overlap integrals and the energies of the SOMOs contribute to the value of ΔE. With these values as inputs, ΔE is −200, −81, and −60 kcal/mol for $CH_3{-}Fe(CO)_3CH_3$, $C_2H_5{-}Fe(CO)_3CH_3$, and $(CH_3)_3C{-}Fe(CO)_3CH_3$, respectively. Though the trend is the same in both cases, there are considerable differences in the magnitudes of the energies calculated using eq 6 and the BDEs calculated by DFT (41.08, 33.91, and 18.21 kcal/mol respectively). DFT calculations of bond energies take into account orbital interaction energies as well as factors such as the deformation energy that lead to a bond energy that can be significantly less than the orbital interaction energy.[35] Thus, DFT calculations of BDEs would be expected to be more accurate than the energies calculated using eq 6.

E. Acyl−Cr Complexes. As indicated in the Introduction, though η^2-acyl−Mo and η^2-acyl−W complexes have been synthesized,[2,4,5] to our knowledge there are no reports of η^2-acyl complexes involving Cr, the lightest group VI metal. The question then arises, should there be stable η^2-acyl−Cr complexes? To address this question, we used the BP86 functional to calculate the energies of the isomers of $CH_3C(O)Cr(CO)_5X$ ($X = I, CH_3$). Although we used a guess for the η^1-$CH_3C(O)Cr(CO)_4CH_3$ structure as the input, the calculation gave the η^2 structure as the final optimized result. Geometry optimization also did not converge to a cis structure for $CH_3C(O)Cr(CO)_5X$ for $X = I$ or CH_3. As such, in Chart 4 only data relevant to the two optimized isomeric structures of $CH_3Cr(CO)_5CH_3$ (trans and η^2) and the three optimized isomeric structures of $CH_3Cr(CO)_5I$ are listed. The η^2 structure is the most stable structure for both complexes. Both the cis and trans isomers of $CH_3Cr(CO)_5X$ are 7-coordinate complexes, which would be expected to be very difficult to prepare. Because the atomic radius decreases in going to lighter group VI transition metals, steric effects would be expected to be more severe for the lightest metal in a 7-coordinate complex, which would be expected to increase the energy of the complex. Thus, it is not surprising that saturated η^2-acyl complexes of Cr have not been reported: They would be expected to be difficult to prepare. As such, we investigated the $CH_3Cr(CO)_4(\eta^3\text{-}C_3H_5)$ complex, which has six ligands. Data on all four isomers were obtained and are listed in Table 6. The complexes are shown in Chart 5 and in Figure 3, where it is clear that the η^2 structure is the most stable. Thus, it would be an interesting challenge to see if an η^2-acylCr complex can be prepared synthetically.

CHART 4

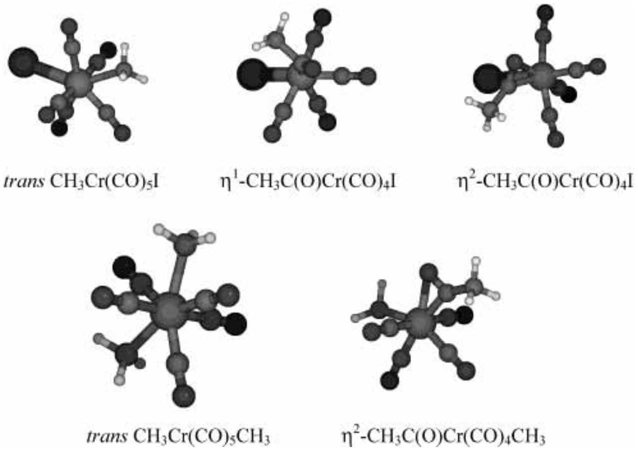
trans $CH_3Cr(CO)_5I$ η^1-$CH_3C(O)Cr(CO)_4I$ η^2-$CH_3C(O)Cr(CO)_4I$

trans $CH_3Cr(CO)_5CH_3$ η^2-$CH_3C(O)Cr(CO)_4CH_3$

TABLE 6: Relative Stability[a,b] of Isomers of Acyl−Cr Complexes

	trans	cis	η^2	η^1
$CH_3Cr(CO)_5I$	0	*c*	−11.15	−9.50
$CH_3Cr(CO)_5CH_3$	0	*c*	−12.45	*c*
$CH_3Cr(CO)_4(\eta^3\text{-}C_3H_5)$	0	−0.60	−8.21	2.35

[a] Energies in kcal/mol. [b] The energy of the trans structure is set to zero and the energies of other structures are reported relative to the trans structure. [c] Geometry optimization did not converge to a structure for this isomer.

CHART 5

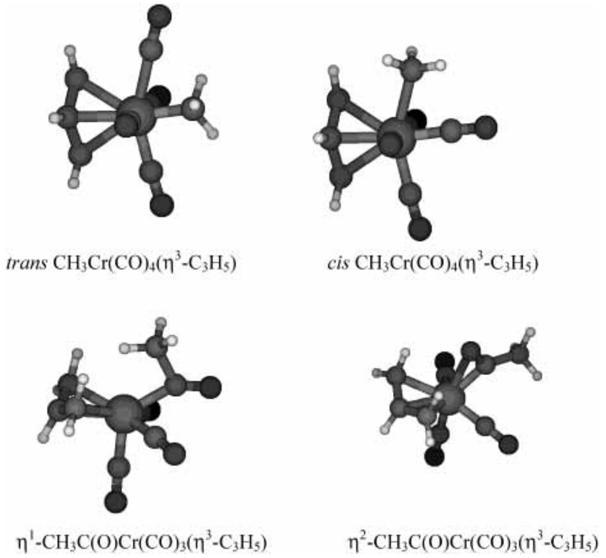
trans $CH_3Cr(CO)_4(\eta^3\text{-}C_3H_5)$ *cis* $CH_3Cr(CO)_4(\eta^3\text{-}C_3H_5)$

η^1-$CH_3C(O)Cr(CO)_3(\eta^3\text{-}C_3H_5)$ η^2-$CH_3C(O)Cr(CO)_3(\eta^3\text{-}C_3H_5)$

IV. Conclusions

DFT methods were used to study η^2-acyl−metal complexes. The BP86 and BLYP functionals gave similar results for the relative energies of the η^1 and η^2-$CH_3C(O)Mn(CO)_4$ complexes. The most stable isomer, $CH_3Mn(CO)_5$, is 9.52 kcal/mol (BLYP) lower than the η^2 isomer. The calculated free energy differences between these complexes are in good agreement with the experimental data of Ford et al.[6]

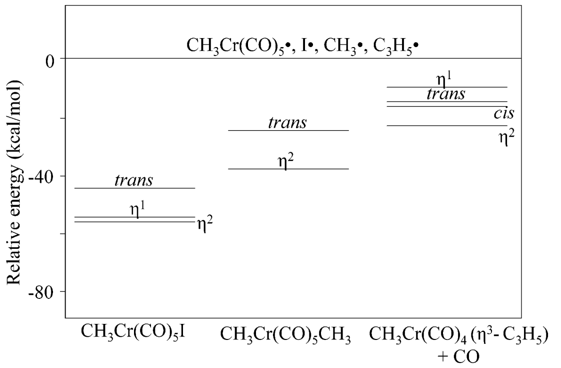

Figure 3. Relative energies of the relevant acyl−Cr complexes where the parent complexes are indicated along the abscissa. The energy origin for the first two complexes corresponds to the separated entities: $CH_3Cr(CO)_4$ and $CH_3Cr(CO)_3 + CH_3$, respectively. For the third complex the energy origin is $CH_3Cr(CO)_5 + C_3H_5$.

In recent calculations Derecskei-Kovacs and Marynick report that the η^1 structure for $CH_3C(O)Mn(CO)_4$ is a transition state. We concur that the structure Derecskei-Kovacs and Marynick present is a transition state. However, we report the structure of another η^1 complex that is a minimum on the potential energy surface, albeit a very shallow minimum at our level of calculations. The existence of even a transient η^1 structure that is an energy minimum leaves open the possibility that it could interact with solvent to form a solvento complex. Whether this actually occurs will depend on the detailed shape of the potential energy surface and the microscopic kinetics operative in this system. Nevertheless, the Mn−THF bond energy in $CH_3C(O)Mn(CO)_4$ (THF) was calculated as 27.60 kcal/mol, and we find that, as shown in Figure 1, the *free energy* difference, calculated using BLYP, between such a complex and the η^2 structure is 2.98 kcal/mol, which is very similar to the estimate for this quantity reported by Ford et al.[6a]

The relative stability of the trans, cis, η^1, and η^2 isomers of $RC(O)Fe(CO)_3X$ ($R = CH_3$, C_2H_5, and $(CH_3)_3C$, $X = I$, H, CH_3) compounds were studied using the BP86 functional. The η^2-$(CH_3)_3CC(O)Fe(CO)_3CH_3$ complex is lowest in energy among its isomers. The energy difference between the η^2 isomer and the η^1 isomer of $RFe(CO)_4I$ is smaller than the corresponding energy difference for the $RFe(CO)_4H$ complexes, with η^2-$RC(O)Fe(CO)_3H$ being more stable than its η^1 isomer.

The energies of the SOMO (singly occupied molecular orbitals) of the $Fe(CO)_3CH_3$ moiety and the relevant alkyl groups (methyl, ethyl, *tert*-butyl) have been calculated. Using a standard molecular orbital approach, interaction energies are consistent with the trend in bond energy for the metal−alkyl bond in alkyl−$Fe(CO)_3CH_3$ complexes that have been calculated using density functional theory. Acyl−Cr complexes were also investigated. η^2-$CH_3C(O)$−$Cr(CO)_4CH_3$ is the most stable structure among its isomers. However, preparation via a 7-coordinated *trans*-$(CH_3)_2Cr(CO)_5$ precursor is likely to be very difficult and may account for the fact that such a complex has not been reported. $CH_3Cr(CO)_4(\eta^3\text{-}C_3H_5)$ avoids the steric impediments associated with a 7-coordinated complex. The η^2 structure of $CH_3Cr(CO)_4(\eta^3\text{-}C_3H_5)$ is the most stable among its isomers and may represent a potential target for synthesis.

Acknowledgment. We acknowledge support of the work by the National Science Foundation under Grant CHE97-34891. We appreciate the help of Dale Braden at Schrödinger Inc. and also thank Dr. David L. Cedeño for helpful discussions and for communicating experimental data on $(C_2H_5)Fe(CO)_4I$ complexes prior to publication.

References and Notes

(1) Blackborow, J. R.; Daroda, R. J.; Wilkinson, G. *Coord. Chem. Rev.* **1982**, *43*, 17.

(2) Durfee, L. D.; Rothwell, I. P. *Chem. Rev.* **1988**, *88*, 1059 and references there in.

(3) Sweany, R. L. *Organometallics* **1989**, *8*, 175.

(4) Skagestad, V.; Tilset, M. *Organometallics* **1992**, *11*, 3293.

(5) (a) Carmona, E.; Contreras, L.; Poveda, M. L.; Sánchez, L. J.; Atwood, J. L.; Rogers, R. D. *Organometallics* **1991**, *10*, 61. (b) Carmona, E.; Contreras, L.; Puebla, E. G.; Monge, A.; Sánchez, L. J. *Organometallics* **1991**, *10*, 71. (c) Carmona, E.; Contreras, L.; Puebla, E. G.; Monge, A.; Sánchez, L. J. *Inorg. Chem.* **1990**, *29*, 700. (d) Rusik, C. A.; Collins, M. A.; Gamble, A. S.; Tonker, T. L.; Templeton, J. L. *J. Am. Chem. Soc.* **1989**, *111*, 2550. (e) Conejo, M. M.; Pizzano, A.; Sánchez, L. J.; Carmona, E. *J. Chem. Soc., Dalton Trans.* **1996**, 3687. (f) Contreras, L.; Pizzano, A.; Sánchez, L. J.; Carmona, E. *J. Organomet. Chem.* **1999**, *582*, 3. (g) Ujaque, G.; Maseras, F.; Lledós, A.; Contreras, L.; Pizzano, A.; Rodewald, D.; Sánchez, L. J.; Carmona, E.; Monge, A.; Ruiz, C. *Organometallics* **1999**, *18*, 3294.

(6) (a) Boese, W. T.; Ford, P. C. *J. Am. Chem. Soc.* **1995**, *117*, 8381. (b) Boese, W. T.; Ford, P. C. *Organometallics* **1994**, *13*, 3525. (c) Boese, W. T.; Lee, B.; Ryba, D. W.; Belt, S. T.; Ford, P. C. *Organometallics* **1993**, *12*, 4739.

(7) Berke, H.; Hoffmann, R. *J. Am. Chem. Soc.* **1978**, *100*, 7224.

(8) Tatsumi, K.; Nakamura, A.; Hofmann, P.; Stauffert, P.; Hoffmann, R. *J. Am. Chem. Soc.* **1985**, *107*, 4440.

(9) (a)Versluis, L.; Ziegler, T.; Baerends, E. J.; Ravenek, W. *J. Am. Chem. Soc.* **1989**, *111*, 2018 (b) Versluis, L.; Ziegler, T. *Organometallics* **1990**, *9*, 2985. (c) Ziegler, T.; Versluis, L. *Adv. Chem. Ber.* **1992**, *125*, 75. (d) Solà, M.; Ziegler, T. *Organometallics* **1996**, *15*, 2611.

(10) Ziegler, T.; Versluis, L.; Tschinke, V. *J. Am. Chem. Soc.* **1986**, *108*, 612.

(11) Margl, P.; Ziegler, T. *J. Am. Chem. Soc.* **1996**, *118*, 7337.

(12) Rappé, A. K. *J. Am. Chem. Soc.* **1987**, *109*, 5605.

(13) Axe, F. U.; Marynick, D. S. *Organometallics* **1987**, *6*, 572.

(14) Derecskei-Kovacs, A.; Marynick, D. S. *J. Am. Chem. Soc.* **2000**, *122*, 2078. And the available geometry data can be accessed via the Internet at http://pubs.acs.org.

(15) D. L. Cedeño and E. Weitz, to be published.

(16) Jaguar 4.0, Schrödinger Inc., Portland, OR, 1998−1999.

(17) Slater, J. C. *The Self-Consistent Field for Molecules and Solids*; Quantum Theory of Molecules and Solids, Vol. 4; McGraw-Hill: New York, 1974.

(18) Becke, A. D. *Phys. Rev. A* **1988**, *38*, 3098.

(19) Perdew, J. P. *Phys. Rev. B* **1986**, *33*, 8822. Perdew, J. P. *Phys. Rev. B* **1986**, *34*, 7406.

(20) Vosko, S. H.; Wild, L.; Nusair, M. *Can. J. Phys.* **1980**, *58*, 1200.

(21) Lee, C.; Yang, W.; Parr, R. G. *Phys. Rev. B* **1988**, *37*, 785.

(22) The LACV3P basis set is a triple-ζ contraction of the LACVP basis set (Hay, P. J.; Wadt, W. R. *J. Chem. Phys.* **1985**, *82*, 299) developed and tested by Schrödinger, Inc.

(23) Deakyne, C. A.; Liebnam, J. F. In *Encyclopedia of Computational Chemistry*; Schleyer, P. v. R., Allinger, N. R., Clark, T., Gasteiger, J., Kollman, P. A., Schaefer, H. F., III., Schreiner, P. R., Eds.; Wiley: Chichester, U.K., 1998; Vol. 2, p 1439.

(24) Boys, S. F.; Bernardi, F. *Mol. Phys.* **1970**, *19*, 553.

(25) Cedeño, D. L.; Weitz, E.; Bérces, A. *J. Phys. Chem. A* **2001**, *105*, 3773.

(26) (a) Tilset, M.; Parker, V. D. *J. Am. Chem. Soc.* **1989**, *111*, 6711. (b) Tilset, M.; Parker, V. D. *J. Am. Chem. Soc.* **1990**, *112*, 2843.

(27) Pearson, R. G. *Chem. Rev.* **1985**, *85*, 41.

(28) Connor, J. A.; Zafarani-Moattar, M. T.; Bickerton, J.; El Saied, N. I.; Suradi, S.; Carson, R.; Al Takhin, G.; Skinner, H. A. *Organometallics* **1982**, *1*, 1166.

(29) Billmers, R.; Griffith, L. L.; Stein, S. E. *J. Phys. Chem.* **1986**, *90*, 517.

(30) Cedeño, D. L.; Weitz, E.; Bérces, A. *J. Phys. Chem. A* **2001**, *105*, 8077.

(31) (a) *Amsterdam Density Functional*, ADF 2001.02 release; SCM, Vrije Universiteit: The Netherlands. (b) Baerends, E. J.; Ellis, D. E.; Ros, P. *Chem. Phys.* **1973**, *2*, 41. (c) Versluis, L.; Ziegler, T. *J. Chem. Phys.* **1988**, *88*, 322. (d) te Velde, G.; Baerends, E. J. *J. Comput. Chem.* **1992**, *99*, 84. (e) Fonseca Guerra, C.; Snijders, J. G.; Baerends, E. J. *Theor. Chem. Acc.* **1998**, *99*, 391.

(32) (a) Snijders, G. J.; Baerends, E. J.; Vernooijs, P. *At. Data Nucl. Data Tables* **1982**, *26*, 483. (b) Vernooijs, P.; Snijders, G. J.; Baerends, E. J. *Slater Type Basis Functions for the whole Periodic System*; internal report; Free University of Amsterdam: Amsterdam, The Netherlands, 1981.

(33) Mawby, R. J.; Basolo, F.; Pearson, R. G. *J. Am. Chem. Soc.* **1964**, *86*, 3994.

(34) Andersen, J.-A. M.; Moss, J. R. *Organometallics* **1994**, *13*, 5013.
(35) Cedeño, D. L.; Weitz, E. *J. Phys. Chem. A* **2002**, *106*, 4651.
(36) Woodward, R. B.; Hoffmann R. *The Conservation of Orbital Symmetry*; Academic Press: New York, 1969.
(37) Albright, T. A.; Burdett, J. K.; Whangbo, M. H. *Orbital Interactions in Chemistry*; Wiley-Interscience: New York, 1985.

(38) Wolfsberg, M.; Helmholtz, L. *J. Chem. Phys.* **1952**, *20*, 837.